*Epilepsia*, 51(8):1628–1632, 2010
doi: 10.1111/j.1528-1167.2010.02570.x

BRIEF COMMUNICATION

# Distribution and proliferation of bone marrow cells in the brain after pilocarpine-induced status epilepticus in mice

*†[1]Beatriz Longo, †[1]Simone Romariz, †Miriam Marcela Blanco, *Juliana Fraga Vasconcelos, *Luciana Bahia, *‡Milena Botelho Pereira Soares, †Luiz E. Mello, and *‡Ricardo Ribeiro-dos-Santos

*Laboratório de Engenharia Tecidual e Imunofarmacologia, CPqGM/FIOCRUZ, Bahia, Brazil; †Laboratório de Neurofisiologia, Departamento de Fisiologia, UNIFESP, São Paulo, Brazil; and ‡Centro de Biotecnologia e Terapia Celular, Hospital São Rafael, Salvador, BA, Brazil

## Summary

**The distribution of bone marrow cells in brain areas during the acute period after pilocarpine-induced status epilepticus (SE) was investigated here. To achieve this, we generated chimeric mice by engrafting bone marrow cells from enhanced green fluorescent protein (eGFP) transgenic mice. GFP$^+$ bone marrow–derived cells were found throughout the brain, predominantly in the hippocampus. As expected, these cells exhibited the characteristics of microglia. The pattern of distribution, proliferation, and differentiation of GFP$^+$ cells changes as a function of intensity and time following SE. This pattern is also a consequence of the inflammatory response, which is followed by the progressive neuronal damage that is characteristic of the pilocarpine model.**

**KEY WORDS: Hippocampus, Chimeric mice, Microglia, Status epilepticus, GFP.**

The occurrence of immunologic dysfunction after seizures has been widely demonstrated (Bernardino et al., 2005; Fabene et al., 2008). Studies from human and experimental epilepsy indicate that after status epilepticus (SE) or epileptic seizures inflammatory cells within the bone marrow cell population have been shown to infiltrate and proliferate in the brain parenchyma, which suggests alterations in immunologic function. Bone marrow–derived cells in the central nervous system (CNS) contribute mostly to the generation of microglia, and the number of microglia that originate from bone marrow increases dramatically after brain damage at the site of injury (Priller et al., 2001; Simard & Rivest, 2004).

Because bone marrow is an accessible source of progenitor cells, the use of these cells has been speculated to treat neurologic diseases in a number of clinical trials. Therefore, the use of bone marrow cell as a possible treatment for neurologic disorders should be carefully evaluated. It is critical to examine first how endogenous bone marrow cells behave and function after the SE. In this study we investigated the migration, proliferation, and microglial nature of bone marrow–derived cells present in the brain at various time points after pilocarpine-induced SE in chimeric mice that were engrafted with bone marrow cells expressing green fluorescent protein (GFP).

## Methods

We transplanted bone marrow from the eGFP transgenic mice into lethally irradiated adult male C57Bl/6 wild-type mice (n = 59). Bone marrow cells were obtained from adult eGFP-donor mice by flushing the femurs and tibiae. Approximately $3 \times 10^7$ cells were administered into each irradiated animal. One month after transplantation, a group of chimeras (n = 44) was injected with pilocarpine (280 mg/kg) to induce SE. Behavioral data were collected during the SE, and the seizures were classified according to a modified version of the Racine scale (Shibley & Smith, 2002). The animals were deeply anesthetized and perfused with 4% paraformaldehyde at the following time points post-SE: 2 h (n = 6), 24 h (n = 6), 48 h (n = 6), 72 h (n = 6), 96 h (n = 6), 7 days (n = 7), or 15 days (n = 7). Before the perfusion, the animals from the 24 h, 7 day, and 15 day groups were administered 5-bromo-2′-deoxyuridine-5′-monophosphate (BrdU, 50 mg/kg) once a day beginning at 30 min of SE onset and ending 2 h before the perfusion. Control chimeric animals (n = 15) were injected with saline and also with BrdU. The brains were removed

Accepted February 19, 2010; Early View publication April 8, 2010.
Address correspondence to Ricardo Ribeiro dos Santos, Centro de Biotecnologia e Terapia Celular, Hospital São Rafael, Av. São Marcos, 2152, São Marcos, CEP: 41.253-190, Salvador- Bahia, Brazil. E-mail: ricardo.ribeiro@hsr.com.br
[1]Longo and Romariz contributed equally to this work.

and processed for immunofluorescence. Sections were incubated with anti-GFP AlexaFluor 488–conjugated (1:600), anti-BrdU (1:500), anti-NeuN (1:200), anti-GFAP (1:200), and anti-Iba1 (1:2,000) antibodies. The sections were then conjugated to the fluorochromes and analyzed using fluorescence and confocal microscopes.

$GFP^+$ cells were counted in 10 random, nonoverlapping fields for all of the time points post-SE (2 h, 24 h, 48 h, 72 h, and 96 h, 7 days, and 15 days) and controls. The same counting protocol was used to estimate the percentage of $BrdU^+$ cells and double-stained $GFP^+/BrdU^+$, $/Iba1^+$, $/NeuN^+$ and $/GFAP^+$ cells in the control, 24-h, 7-d, and 15-d, groups. Cells were counted in six selected brain areas: neocortex, piriform cortex, hippocampus, thalamus, subventricular zone in the lateral ventricle wall (SVZ), and choroid plexus. Analysis of variance (ANOVA) followed by Tukey-Kramer or Mann-Whitney post hoc tests were used for statistical analysis.

## Results

Although there was a low number of $GFP^+$ cells in the control chimeric animals, a significant increase of the $GFP^+$ cells was observed in the brain after SE ($p < 0.05$). The number of these cells gradually increased at different time points after SE (2 h, 24 h, 48 h, 72 h, 96 h, 7 days, and 15 days) ($p < 0.001$). The $GFP^+$ cells began increasing in frequency by 48 h and continued increasing until 15 days after SE, which was the last time point examined (supporting information). The hippocampus had the largest number of $GFP^+$ cells, followed by the choroid plexus and thalamus ($p < 0.001$). The $GFP^+$ cells were concentrated in the hilus, CA1, and CA3. In addition, more $GFP^+$ cell clusters were observed in caudal levels of the ventral hippocampus than in the dorsal hippocampus. The number of bone marrow–derived $GFP^+$ cells in the brain was also influenced by the severity of SE based on a Racine modified scale. Fifty-four percent (precisely 54.3%) of the total number of $GFP^+$ cells was found in animals with the highest scores (4 and 5) and 25.5% was present in animals with a score of 3. Scores 1 and 2 were excluded from this analysis.

By counting the number of $GFP^+/BrdU^+$ and $GFP^-/BrdU^+$ (only BrdU) cells in the control and SE animals at 24 h, 7 days, and 15 days after SE, we evaluated bone marrow cells and endogenous cell proliferation, respectively. High levels of $GFP^-/BrdU^+$ cells were present in the

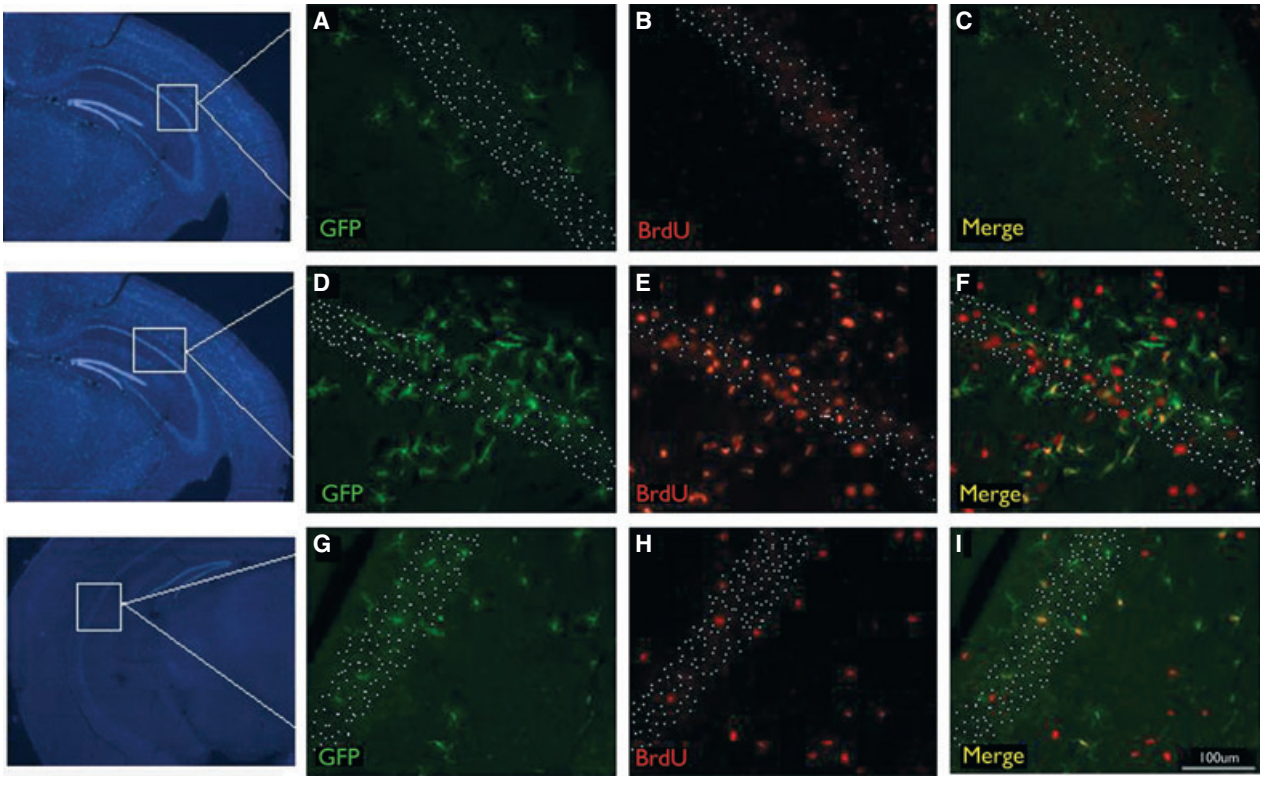


**Figure 1.**
$GFP^+$ and $BrdU^+$ stained cells in the hippocampus (CA1) of chimeric animals. Images show $GFP^+$ cells in green, $BrdU^+$ cells in red, and double-stained $GFP^+/BrdU^+$ cells as merge images (orange) at 24 h (**A–C**), 7 days (**D–F**), and 15 days (**G–I**) after status epilepticus (SE). Squares in DAPI images of the hippocampus indicate the level of $GFP^+/BrdU^+$ cells in CA1. Dashed lines indicate the CA1 pyramidal cell layer. Magnification of 20× in A-I and 2× for DAPI.

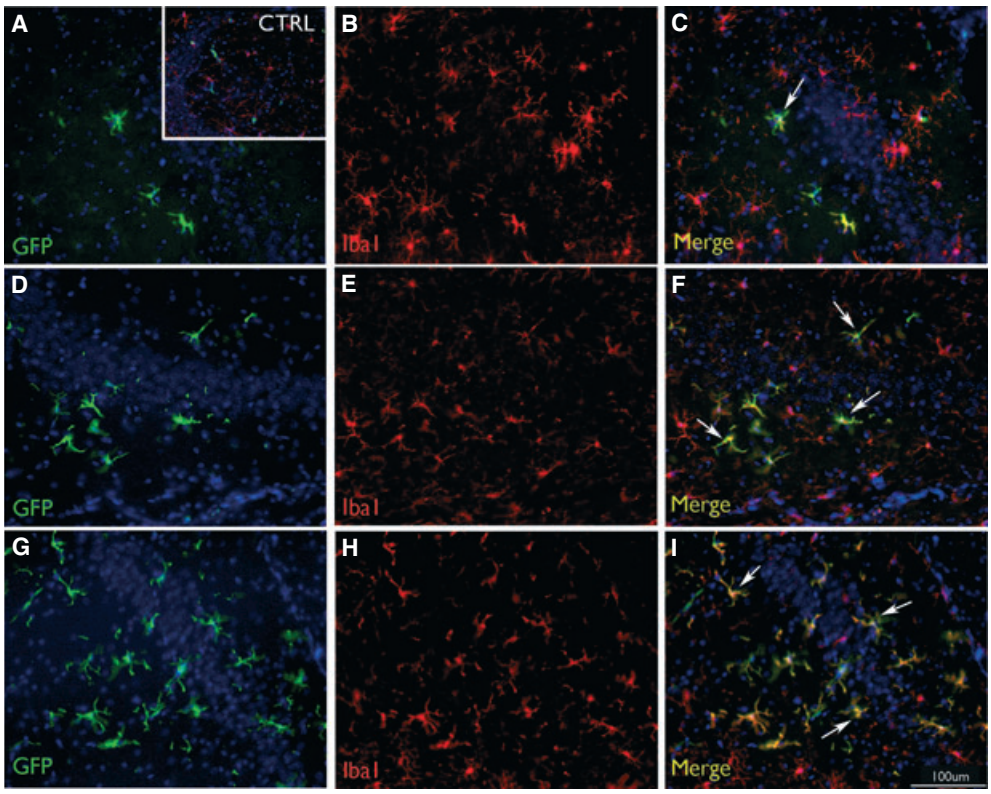


**Figure 2.**
$GFP^+$ (green) in $Iba1^+$ (red) in cell population in the hippocampus (CA3) of chimeric animals at 24 h (**A–C**), 7 days (**D–F**), and 15 days (**G–I**) after status epilepticus (SE) (in **A**: detail of a control animal with very few $GFP^+$ cells). Double-stained cells ($Iba1^+/GFP^+$) are indicated in merge images (arrows). Cells were counterstained with DAPI (blue) for nuclear staining. Magnification of 20×.


hippocampus, SVZ, and choroid plexus of SE mice at 7 days, but they decreased at 15 days ($p < 0.001$). In the hippocampus, no $GFP^+/BrdU^+$ cells were present in the control group, very few were present in the 24 h group, and the number of cells increased approximately 10-fold by days 7 and 15 (Fig. 1). Despite this increase, the $GFP^+/BrdU^+$ cells represented a small proportion (approximately one-third) of the total number of $GFP^+$ cells. By 24 h after SE, the $GFP^+/BrdU^+$ cells represented 12.8% of the total. By days 7 and 15, the $GFP^+/BrdU^+$ cells represented 28.5% and 23.7% of the total, respectively, which indicates a delay in proliferation after bone marrow $GFP^+$ cell migration.

Qualitative immunofluorescence analyses to evaluate whether the $GFP^+$ cells expressed microglia (Iba1), astrocyte (GFAP), or neuronal (NeuN) markers indicated that endogenous microglia expressing Iba1 were detected in the controls and in the SE animals. In the controls, no co-localization of $Iba1^+$ with $GFP^+$ cells was observed. However, subsequent to SE, the percentage of double-stained $GFP^+/Iba1^+$ cells increased over time, and coincided with the temporal pattern of bone marrow–derived $GFP^+$ cell migration and proliferation. At later time points, the majority of the $GFP^+$ cells observed in the epileptic groups expressed Iba1 (Fig. 2). The percentages of $GFP^+/Iba1^+$ within the $Iba1^+$ population at 24 h, 7 days, and 15 days were 2.8%, 23.1%, and 44.7%, respectively. The same distribution pattern of microglia and co-localized $GFP^+$ cells was observed in the hippocampus (0.3%, 8.9%, and 24.5%, respectively). We did not observe $GFP^+$ cells developing astrocytic or neuronal phenotypes, which would have been indicated by double-staining for $GFP^+$ and $GFAP^+$ or $NeuN^+$.

Correlation analyses were performed between the time after SE and the presence of $GFP^+$, $BrdU^+$, and $Iba1^+$ cells in the hippocampus. A significant correlation was noted between $GFP^+$ cells and time after SE. The number of $GFP^+$ cells as well as double-stained $GFP^+/BrdU^+$ and $Iba^+/GFP^+$ cells in the hippocampus increased as time after SE increased. Significant correlations were also observed between SE intensity and the number of $GFP^+$ and $GFP^+/BrdU^+$ cells. The more severe the SE, the greater the number of $GFP^+$ and $GFP^+/BrdU^+$ cells. A negative correlation was found between the time after SE and $Iba1^+$; as time passed, the number of $Iba1^+$ stained cells decreased (supporting information).

## Discussion

The gradual migration of bone marrow–derived cells in the chimeric brain began immediately after SE induction and continued for at least 15 days, whereas the proliferation of these cells and their microglial phenotype began later (7 days and 15 days). At all times after SE the majority of $GFP^+$ cells concentrated in the hippocampus. This preferential concentration of bone marrow–derived cells may result from the type of seizure induced by the pilocarpine model, which damages the hippocampus predominantly (Mello et al., 1993).

Interestingly, the majority of bone marrow–derived cells present in the brain exhibited the characteristics of microglia during the first and second weeks following SE, although the increase did not occur in the first 24 h. Endogenous microglia were already numerous a few hours after SE (2–24 h) but they were not derived from the transplanted bone marrow ($GFP^-$). The bone marrow–derived cells expressing the microglial marker ($GFP^+/Iba1^+$) appeared 7 days and 15 days following SE. These findings suggest a biphasic nature of microglia according to which microglia already present at the inflammation site are recruited during the first 24 h after SE, followed by the migration of bone marrow–derived microglia to the damaged tissue during the first and second weeks after SE. Recent studies have shown that bone marrow–derived and CNS resident microglia cells possess different properties and kinetics (Napoli & Neumann, 2009). Moreover, articles reviewing microglial function in the CNS have proposed that microglia serve a dual role in neurogenesis and inflammation depending upon the balance between secreted molecules with pro- and anti-inflammatory action and on the physiologic situation (Monje et al., 2003; Ekdahl et al., 2009). There is evidence of both protective (Albensi, 2001) and toxic (Vezzani et al., 2000; Borges et al., 2004) roles of the inflammatory response elicited following seizures to control the patterns of neuronal loss and replacement associated with seizures.

In summary, the temporal migration, distribution, and proliferation patterns of bone marrow–derived cells in the brain after SE were modified as part of the inflammatory response that occurs following progressive brain injury characteristic to this model. Whether these bone marrow–derived cells have degenerative or regenerative effects on seizure-induced damage is still unclear. Our study helped clarify some important issues regarding bone marrow–derived cells in seizure and may contribute to develop novel and reliable cell-based therapies in the future.

## Acknowledgments

We apologize to all whose works were not cited due to space limitations. We are grateful to Jaqueline Noronha, Maria Fernanda Valente, Enéas Ferrazolli, and Thomas Perlaky for the technical support; Yiwei Jia and Willy Hausner for the help with confocal images; and Dr. Daniel Peterson for the critical comments. This work was supported by FAPESB, FAPESP, CNPq, and FIOCRUZ.

## Disclosure

We confirm that we have read the Journal's position on issues involved in ethical publication and affirm that this report is consistent with those guidelines. None of the authors has any conflict of interest to disclose.

## References

Albensi BC. (2001) Models of brain injury and alterations in synaptic plasticity. *J Neurosci Res* 65:279–283.

Bernardino L, Ferreira R, Cristovao AJ, Sales F, Malva JO. (2005) Inflammation and neurogenesis in temporal lobe epilepsy. *Curr Drug Targets CNS Neurol Disord* 4:349–360.

Borges K, McDermott D, Dingledine R. (2004) Reciprocal changes of CD44 and GAP-43 expression in the dentate gyrus inner molecular layer after status epilepticus in mice. *Exp Neurol* 188:1–10.

Ekdahl CT, Kokaia Z, Lindvall O. (2009) Brain inflammation and adult neurogenesis: the dual role of microglia. *Neuroscience* 158:1021–1029.

Fabene PF, Navarro Mora G, Martinello M, Rossi B, Merigo F, Ottoboni L, Bach S, Angiari S, Benati D, Chakir A, Zanetti L, Schio F, Osculati A, Marzola P, Nicolato E, Homeister JW, Xia L, Lowe JB, McEver RP, Osculati F, Sbarbati A, Butcher EC, Constantin G. (2008) A role for leukocyte-endothelial adhesion mechanisms in epilepsy. *Nat Med* 14:1377–1383.

Mello LE, Cavalheiro EA, Tan AM, Kupfer WR, Pretorius JK, Babb TL, Finch DM. (1993) Circuit mechanisms of seizures in the pilocarpine model of chronic epilepsy: cell loss and mossy fiber sprouting. *Epilepsia* 34:985–995.

Monje ML, Toda H, Palmer TD. (2003) Inflammatory blockade restores adult hippocampal neurogenesis. *Science* 302:1760–1765.

Napoli I, Neumann H. (2009) Microglial clearance function in health and disease. *Neuroscience* 158:1030–1038.

Priller J, Flugel A, Wehner T, Boentert M, Haas CA, Prinz M, Fernandez-Klett F, Prass K, Bechmann I, de Boer BA, Frotscher M, Kreutzberg GW, Persons DA, Dirnagl U. (2001) Targeting gene-modified hematopoietic cells to the central nervous system: use of green fluorescent protein uncovers microglial engraftment. *Nat Med* 7:1356–1361.

Shibley H, Smith B. (2002) Pilocarpine-induced status epilepticus results in mossy fiber sprouting and spontaneous seizures in C57BL/6 and CD-1 mice. *Epilepsy Res* 49:109–120.

Simard AR, Rivest S. (2004) Bone marrow stem cells have the ability to populate the entire central nervous system into fully differentiated parenchymal microglia. *FASEB J* 18:998–1000.

Vezzani A, Moneta D, Conti M, Richichi C, Ravizza T, De Luigi A, De Simoni MG, Sperk G, Andell-Jonsson S, Lundkvist J, Iverfeldt K, Bartfai T. (2000) Powerful anticonvulsant action of IL-1 receptor antagonist on intracerebral injection and astrocytic overexpression in mice. *Proc Natl Acad Sci U S A* 97:11534–11539.

## Supporting Information

Additional supporting information may be found in the online version of this article:

**Table S1.** Listing of correlations.

**Figure S1.** Quantitative assessment of green fluorescent protein–positive ($GFP^+$) cells in the brain of chimeric mice. The increasing number of $GFP^+$ cells in status epilepticus (SE) (as black square) at each time point along 15 days after SE—2 h (n = 6), 24 h (n = 6), 48 h (n = 6), 72 h (n = 6), 96 h (n = 6), 7 days (n = 7), or 15 days (n = 7)—was compared to the control (n = 15), which is represented as an opened square (*$p < 0.001$ vs. control group).

**Figure S2.** Distribution of degenerating neurons after status epilepticus (SE). Fluoro-Jade B–positive neurons in the neocortex (A, D), pyramidal layer of CA1 in the hippocampus (B, E), and thalamus (C, F) of respectively 8 h, 7 days, and 15 days after SE (magnification of 20× in A, B, and C and 40× in D, E, and F).

**Figure S3.** Expression of glial and neuronal markers 7 days after status epilepticus (SE). Images show green fluorescent protein–positive ($GFP^+$) cells (green) counterstained with 4′,6-diamidino-2-phenylindole (DAPI) (blue) for the nuclear staining (A, C, D, F, G, and I) in the neocortex. $CD11b^+$ (B and C), $GFAP^+$ (E and F), and $NeuN^+$ (H and I) cells were stained in red. In C, F, and I images were merged. Arrows indicated $GFP^+CD11b^+$ cells in C. Magnification of 20×.

**Figure S4.** Confocal image of BrdU (red) and green fluorescent protein (GFP) (green) merged cells in the hippocampal area 7 days after status epilepticus (SE). Note microglial morphology of donor-derived $GFP^+$/BrdU labeled cells. (magnification of 60×, Olympus FV100).

Please note: Wiley-Blackwell is not responsible for the content or functionality of any supporting information supplied by the authors. Any queries (other than missing material) should be directed to the corresponding author for the article.